International Atomic Energy Agency

INDC(SEC)-68/G+Sp.

INDC INTERNATIONAL NUCLEAR DATA COMMITTEE

CONSOLIDATED PROGRESS REPORT FOR 1977-78

ON NUCLEAR DATA ACTIVITIES

OUTSIDE THE NDS SERVICE AREA

Austria

Netherlands

Switzerland

January 1979

IAEA NUCLEAR DATA SECTION, KÄRNTNER RING 11, A-1010 VIENNA

Reproduced by the IAEA in Austria
January 1979

79-00713

INDC(SEC)-68/G+Sp.

CONSOLIDATED PROGRESS REPORT FOR 1977-78

ON NUCLEAR DATA ACTIVITIES

OUTSIDE THE NDS SERVICE AREA

Austria

Netherlands

Switzerland

January 1979

FOREWORD

This consolidated progress report has been compiled from reports received in summer 1978 from countries outside the NDS service area. A second report, INDC(SEC)-67/L, covers countries within the NDS service area.

The report is arranged alphabetically by country, and reproduces the content of each individual report as it was received by the INDC Secretariat. Progress reports of other countries which have received already wide distribution, are not reproduced in this report.

As in all progress reports the information included here is partly preliminary and is to be considered as private communication. Consequently, the individual reports are not to be quoted without the permission of the authors.

Table of Contents

PROGRESS REPORT TO INDC AND NEANDC FROM AUSTRIA

April 1977

O.J.Eder, Editor

This report contains abstracts about work performed at

Atominstitut der Österreichischen Universitäten, Wien

Institut für Radiumforschung und Kernphysik der Österreichischen Akademie der Wissenschaften, Wien

Institut für Theoretische Physik und Reaktorphysik der Technischen Universität Graz

Österreichische
Studiengesellschaft
für Atomenergie
A-2444 Seibersdorf
Austria

ATOMINSTITUT DER ÖSTERREICHISCHEN UNIVERSITÄTEN, WIEN

1. NEUTRON SOURCES AND NEUTRON DETECTION

1.1 Measurement of the emission spectra of Sb-Be, Ga-D_2O, In-Be, Mn-Be and Ga-Be photoneutron sources

E.Zankl, F.Bensch

The energy distribution of the photoneutrons produced in said sources was measured by a proton-recoil proportional counter. The sources were surrounded by spherical lead-shields to reduce the very intense gamma field. Various methods of (n,γ)-discrimination were investigated and the best results were obtained by an electronic division method which used the quotient of the rise-time to the pulse heigt of each pulse. The experimental results showed for the Sb-Be source that there exists also a continuous neutron contribution, produced by the $^9Be(\gamma,n)2\alpha$-reaction, besides the sharp neutron peak at 24keV. Good agreement with earlier theoretical calculations was obtained for the Ga-D_2O sources. For the first time there exist accurate measurements of the energy distribution of In-Be, Mn-Be and Ga-Be photoneutrons; these sources have several neutron groups with discrete energies.

2. NEUTRON SCATTERING

2.1 Electric and Nuclear Scattering of Slow Neutrons by Atoms

G.Eder

The electric scattering of neutrons by the Coulomb field of the nucleus and the electrons of a free, neutral and non-magnetic atom is due to the internal charge distribution, the magnetic moment, and the electric polarizability of the neutron. The interference between electric and nuclear interaction of slow neutrons ($l = 0$) is discussed. Expressions for differential cross sections and final state polarization are derived. The electric polarizability modifies essentially the left-right asymmetry of the scattering cross section for polarized neutrons.

2.2 Parameter Systematic for a Neutron-Nucleus Optical Potential*)

G.Eder, H.Leeb and H.Oberhummer

The functional relations between the potential depth and the half density radius of the phenomenological optical neutron-nucleus potential are studied. Parameter systematics for the energy range from 4MeV to 30MeV are constructed which include this ambiguity. It is demonstrated that besides the usually assumed isospin dependence of the real potential depth there must also exist a dependance on the mass number of the target nucleus. The work confirms once more shell effects in the surface absorption term and suggests a method to separate volume and surface absorption by their energy dependence.

*)The work is partly supported by Kulturamt der Stadt Wien.

3. NEUTRON INTERFEROMETRY

3.1 Measurements of Scattering Lengths by Neutron Interferometry

H.Rauch, U.Bonse*, W.Bauspiess**, H.Kaiser, G.Badurek

The perfect crystal neutron interferometer which was developed during the last years (Phys.Lett. A47 (1974) 369) is used for high precision measurements of coherent scattering lengths of various gases. The measurements are carried out at the high flux reactor in Grenoble. The results serve for a deeper understanding of nuclear-, electromagnetic- and few-body-interaction (Proc.Gatlinburg CONF-760601-P2, p. 1094 (1976) and Proc.Lowell CONF-760715-P2, p. 1027). We got the following values for the bound coherent scattering length (in 10^{-13}cm):

Al	3.449 ± 0.005	H	−3.42 ± 0.03
Bi	8.502 ± 0.012	He	3.007 ± 0.03
Mg	5.375 ± 0.003	N	8.975 ± 0.07
Nb	7.054 ± 0.003	O	5.735 ± 0.05
Sn	6.228 ± 0.004	Ar	2.017 ± 0.02
V	−0.382 ± 0.001		
Zn	5.686 ± 0.003		

3.2 Magnetic Effects in Neutron Interferometry

H.Rauch, U.Bonse*, A.Zeilinger, G.Badurek, W.Bauspiess**, H.Kaiser, W.Schindler

---

* Institut für Physik, Universität Dortmund
** Institut für Physik, Universität Dortmund and Institut Laue-Langevin, Grenoble

The neutron interferometer is sensitive to nuclear and magnetic phase shifts as well. After we have verified the 4π-periodicity for spinor rotation (Phys.Lett. 54A (1975) 425) new modulation and polarization effects are observed for simultaneous nuclear and magnetic phase shifts (Phys.Rev. D14 (1976) 1177; Nuovo Cim.34B (1976) 76). New neutron interferometric measurements with an advanced magnetic field positioning yield an accuracy of about 2% for the 4π-factor and about 1% for the determination of magnetic forward scattering lengths. Experiments with polarized incident neutrons are in preparation.

4. NEUTRON DEPOLARIZATION

4.1 Search for Magnetic Order in Selected Pseudobinary Systems down to Milli Kelvin Temperatures

R.Goblirsch, H.W.Weber, G.Hilscher*, R.Grössinger*, W.Steiner**

Magnetization and neutron depolarization experiments performed on the pseudobinary systems $Y_6(Fe_xMn_{1-x})_{23}$, $Zr(Fe_xCo_{1-x})_2$ and $Y(Fe_xAl_{1-x})_2$ are reported. At some intermediate concentrations bulk magnetization measurements did not show a Curie temperature down to 2K. Neutron depolarization measurements down to 30mK confirm the absence of any spontaneous order in these systems. However, the magnetization curves obtained indicate the existance of magnetic clusters. This assumption is supported by the appearance of a field induced magnetic short range order observed by neutron depolarization experiments. The results are discussed in terms of a simple cluster model.

4.2 Instrumental Developments in Polarized Neutron Research

G.Badurek, H.Rauch, J.Hammer

A fully transistorized electronic spin-flip chopper system for polarized neutron beams based on a modified Mezei spin-flip device could be developed, which represents an improved version of the originally described DC flipper-chopper (Nucl.Instr.Meth. 128 (1975) 315) and provides a quasi elastic time resolution in the 1µs range and a minimum pulse width of about 3 - 5µs. Feasibility studies on the application of the pseudo-statistical correlation method for that type of chopper clearly showed the disturbing influence of systematical errors introduced by deviations of the modulation function from their mathematically ideal value. The conclusion could be drawn that the correlation technique is useful only for moderate resolution, i.e. elementary pulse widths of more

* Institut für Experimentalphysik, TU Wien
** Institut für Angewandte Physik, TU Wien

than 20µs, and low modulation depth as it is frequently the case, if spin-dependent scattering is investigated only without the use of an analysing crystal.
A further development is concerned with the extension of the well established neutron depolarization method to dynamic process and relaxation phenomena. At present the electronic setup for the pulsed analyzation has been completed and a search for magnetic after-effects in Dy single and polycrystals is in progress.

5. NEUTRON DIFFRACTION

5.1 Fourier Neutron TOF-Diffractometry

G.Badurek, G.P.Westphal, P.Ziegler

A computer controlled time-of-flight diffractometer for thermal neutrons has been developed (Atomkernenergie 29 (1977) 27), allowing efficient use of the available intensity. An especially designed so-called Fourier-chopper modulates the incident polychromatic beam periodically in time with different frequencies. From the frequency dependent count rate the Fourier transform of the TOF distribution of the scattered neutrons is derived by means of a four-quarter-period phase sensitive detector system. This distribution containing the structural information of the scattering sample can be obtained by performing the corresponding inverse transformation by means of a computer program. The safe maximum rotational speed of the chopper rotor is about 11000 rpm, corresponding to a maximum modulation frequency of the beam of 100kHz. The time resolution of the instrument for a flight path length of 1 - 2m is of the order of 1%. It could be shown (Nucl. Instr. Meth. 137 (1976) 595) that the presence of the higher harmonics in the nearly triangular chopper modulation function causes only negligible systematic errors in the determination of the Fourier components of the neutron TOF-distribution, thus making complicated stator shaping procedures for sinusoidal modulation not necessary. Preliminary test measurements on poly- and single crystal specimens could demonstrate the correct function of the instrument.

5.2 Development of a new Small-Angle X-Ray and Neutron Diffractometer

D.Bader, H.Rauch, A.Zeilinger

A perfect crystal diffractometer for the study of small-angle diffraction was developed. The device is both applicable to X-ray and neutron diffraction. Therefore measurements with these radiations on the same sample with the same geometry are possible. The angular

resolution is in the order of seconds of arc. An optical control system was constructed which is only sensitive to the relative position of the two monochromators and therefore measures the parallelity and deviations from parallelity of these two crystals.

6. NEUTRON RADIOGRAPHY

6.1 Neutron Radiographic Measurements of the Diffusion of H in Metals

W.A.Pochman, A.Zeilinger

Neutron radiography was used to measure hydrogen diffusion in metals (J.Appl.Phys. 47 (1976) 5478; J.Phys.F: Metal.Phys., in print). It is possible to work in a range of exposures where the optical density distribution on the radiographic film directly represents the hydrogen distribution in the sample. The method is essentially non-destructive and the hydrogen need not penetrate surfaces during the measurement. The diffusion coefficients of H in α-Ti, V, Nb and Ta in qualities as usually delivered were measured for temperatures between 50 to 110°C. The results indicate that the diffusion coefficient of H in β-Ti, Nb and Ta is not very sensitive to chemical composition and impurity content. It is concluded that for most technical applications regarding the H transport properties it is not necessary to use extremely pure metals.

6.2 Neutron Radiography of TRIGA Fuel Rods

C.Koberger, W.A.Pochman, H.Rauch, A.Zeilinger, H.Böck

Neutron radiographic investigations of fresh TRIGA fuel rods showed cracks in two elements running right through the fuel briquette. As the new elements were not radioactive, the radiographs could be taken with Gd-foils using the direct method (Atomkernenergie 29 (1977) 231). After the exposition time of several minutes the fuel elements became slightly radioactive showing a radiation level of 100mrem/h measured on contact immediately after radiographing. This activity decayed within a few hours. Further measurements of irradiated fuel elements using the track etch technique are under progress.

INSTITUT FÜR RADIUMFORSCHUNG UND KERNPHYSIK DER
ÖSTERREICHISCHEN AKADEMIE DER WISSENSCHAFTEN, WIEN

1. Precise measurement of the $^{63}Cu(n,\alpha)^{60}Co$ cross section with 14MeV neutrons

G.Winkler

The $^{63}Cu(n,\alpha)^{60}Co$ reaction is a crucial fluence monitor in reactor dosimetry and it is of great importance in unfolding the high-energy part of neutron spectra by foil activation techniques. As significant discrepancies axist in the literature data the $^{63}Cu(n,\alpha)$ cross section has been remeasured with 14 MeV neutrons with an accuracy of a few per cent.

2. Activation Analysis Applications in Archaeology

W.Czerny, G.Winkler

The use of 14MeV neutrons for the analysis of ancient pottery has been investigated. A comparison technique using Al-foils as a standard was introduced. The main components Si, Al, Mg and Fe could be evaluated within a short time with an error of a few per cent thus differentiating between samples of different origin. It has been shown that also the analysis of minor components in pottery such as Na, Ca, Sc, Ti, Mn, Ni, As, Rb, Y, Zr, Cs,Ce can be performed by activation with fast neutrons with moderate precision using a Ge(Li)γ-spectrometer system. The work will be published in the Journal of Radioanalytical Chemistry.

3. Measurement of differential elastic and inelastic scattering cross sections with 14MeV neutrons on elements of practical importance

K.Hansjakob, G.Staffel, G.Winkler, F.Wenninger,
A.Chalupka, H.Vonach

Using time-of-flight techniques for neutron spectroscopy a program has been started to measure the elastic scattering cross sections $(\frac{d\sigma}{d\Omega})_{el}(\theta)$ in the region $\theta = 20^{o} - 135^{o}$ with an accuracy of about 10%, the high energy part of the inelastic neutron spectra $(\frac{\delta^2\sigma}{\delta E_n \cdot d\Omega}(\theta))$ as a function for θ and $E_n' = 3 - 14$MeV with an energy resolution of about 0.5MeV. In the beginning emphasis is

laid on measurements on Ba in its natural isotopic composition and on measurements of the cross sections for forming the first 2^+ level of ^{138}Ba. Furthermore measurements of the low-energy part of the neutron spectra from (n,n')- and (n,2n)-reactions in the region $E_{n'}$ = 0.5 - 3MeV averaged over 6 are plannad.

4. Multiparameter-coincidence study of the reaction Zn(n,n'γ) at 14MeV

H.Kratschmar, S.Tagesen

A sample of natural Zn has been irradiated with 14MeV neutrons from a nanosecond pulsed beam facility. Coincidence-events have been recorded as 3-word items containing neutron time-of-flight, recoil energy (in NE 213) and γ-ray energy (Ge(Li)-detector). Neutron energy spectra for transitions to the first excited levels of ^{64,66,68}Zn will be extracted and compared to results of statistical model calculations.

5. On the low-energy performance of the Munich PSD system

A.Chalupka and G.Stengl
M.R.Maier* and P.Sperr*

The performance of the Munich pulse-shape discrimination (PSD) circuit was tested at very low particle energies. n-γ separation turned out to be possible down to $E_{el} \approx 30$keV also for relatively large (5"ø x 1") NE 213 scintillators. Even at the lowest energies rejection of 99% of the γ-pulses could be achieved if a loss of about 30% of the neutron pulses was permitted.
(Will be published in Nucl.Instr. and Meth.)

6. Temperature dependence of the pulse shape discrimination properties of NE 213

A.Chalupka, G.Stengl and H.Vonach

The temperature dependence of the pulse shape discrimination (PSD) properties of the liquid scintillator NE 213 was investigated in the temperature range -15° - +30°C. The large temperature dependence of the PSD properties reported in the literature could not be confirmed. Even in very sensitive measurements no change in the PSD properties was observable. This indicates that both intensity ratio of the fast and slow components of the scintillation and the scintillation decay times have very small temperature coefficients.
(Will be published in Nucl.Instr.and Meth.)

---

* Physikdepartment, TU München

7. Statistical and optical model calculations of neutron induced reaction cross sections for $^{134-138}Ba$*

B.Strohmaier and M.Uhl

Average neutron induced reaction cross sections for $^{134-138}Ba$ for incident energies between 20keV and 20MeV have been calculated by means of the optical and the statistical model with consideration of preequilibrium emission. The calculations comprise the total, the nonelastic, the differential elastic, the (n,γ), $(n,x n\gamma)$, $(n,p\gamma)$, $(n,pn\gamma)$ and $(n,np\gamma)$ cross sections, as well as the production spectra of neutrons, protons and gamma-rays. For the model calculations a consistent set of parameters based on experimental data as far as possible was employed. The accuracy of the calculated cross sections was estimated.

8. Statistical model calculations of neutron induced cross sections for ^{31}P*

B.Strohmaier and M.Uhl

Average $(n,x n\gamma)$, $(n,\gamma\gamma)$, $(n,pn\gamma)$, $(n,np\gamma)$, $(n,\alpha\gamma)$, $(n,\alpha n\gamma)$ and $(n,n\alpha\gamma)$ cross sections as well as particle and gamma-ray production spectra for ^{31}P have been calculated for incident energies between threshold and 20MeV. Preequilibrium emission was accounted for. Good agreement between computed and experimental cross sections could be achieved by use of a single set of model parameters.

9. Measurement of energy spectra and angular distributions of charged particles emitted in nuclear reactions induced by 14MeV neutrons

P.Hille, M.Uhl, K.Richter, C.Derndorfer, R.Nowotny, G.Stengl

Measurement of the reaction $^{56}Fe(n,\alpha)$ has been completed and compared to statistical model calculations. The new improved version of the cylindrical multiwire chamber is now tested.

10. Age-determination of bones by activation with 14MeV neutrons

P.Hille, H.Vonach, P.Eisenbarth

In cooperation with the Palaeontological Institute of the University of Vienna the N/P- and F/P-ratios of fossil bones are determined by activation analysis and compared to age determination by other methods. Work is now concentrated on bone material found in Austrian caves.

---

* Work supported by the European Communities (EURATOM)

11. Measurement of γ-multiplicities after (n,n')-reactions with 14MeV neutrons

P.Grabmayr, P.Hille

The project described in the last report has been started by calibrating the γ-detector using inelastic 2 - 3MeV neutron scattering on Li-, Si- and Fe-targets.

12. Neutron sputtering

G.Stengl, P.Hille

Using the pulsed high intensity neutron generator at the Institut für Radiumforschung it is planned to study 14MeV neutron sputtering of several materials. TOF-technique will be used for mass identification of sputtered atoms and compounds. Neutron sputtering is an important problem for the development of fusion reactors.

INSTITUT FÜR THEORETISCHE PHYSIK UND REAKTORPHYSIK DER TECHNISCHEN UNIVERSITÄT GRAZ

1. On the Determination of the Resonance Selfshielding in Materials of Medium Atomic Weight*

M.Heindler

In the present study the theoretical basis for a computer code (SEFAC) has been worked out that allows for resolved resonances the correct calculation of the energy- and temperature dependence on cross-sections, on non-shielded and effective group cross-sections and on resonance selfshielding factors of medium-heavy elements.

With the help of this programme and a set of resonance parameters for iron, evaluated by Le Coq and Ribon, the cross-sections and the selfshielding factors for the radiative capture in iron have been calculated, dependent on the energy of the neutrons, on the temperature of iron, the form of the neutron spectre in the regarded reactor type, and on the dilution cross-section of the iron in the considered reactor zone.

The data gained by this programme SEFAC for the effective group

---

* Habil. T.U. Graz, 1976

cross-sections and the selfshielding factors of medium heavy elements will enter into the version IV of the CADARACHE-cross-section data files, which will be made use of when projecting the fast 1200MWe reactor "Super Phénix".

2. Diffusiontheoretical Treatment of Coupled Cores*

H.Rabitsch

The associated flux distributions of weakly coupled slab- and cylindergeometrical cores are calculated by applying the one-group diffusion theory. From the integral representation of the neutron flux by its boundary values the explicit terms of the associated flux distributions for approximately calculated boundary fluxes are derived. A first order perturbation theory makes it possible to determine the buckling change and the resulting flux distributions of coupled systems from the associated flux distributions. The buckling changes are evaluated for coupled cores in slab geometry and for cores of a cross-section in circular ring sector shape; their results are compared with each other.

3. Transporttheoretical Treatment of Spherically Symmetric Cores*

H.Hubmer

From the view of reactor safety the fine structure of the flux in a light water-cooled statistical pebble bed reactor is of considerable interest. Calculation models are applied to make the use of analytical methods possible - e.g. one considers the neighbouring sphere of a reference sphere as distributed on a concentric shell. The applicability of integrodifferential as well as of integral transport theoretical methods on the model of spherically symmetric assembled cores is to be investigated.

4. The Second Order Correlation Functions of the Neutron Field Dealt with in the n-Group Diffusion Theory

E.Ledinegg

Beside the direct method of incore spectroscopy there are also integral methods of interest that can be used for testing multigroup parameters. For reactors of low power also stochastic methods can be applied which refer to the inner pile noise, respectively to the correlation behaviour of neutron chains of the same or different energy groups.

In the present study the cross- and autocorrelation function of two optionally chosen energy groups are calculated; only statistical

---

* Diss. T.U. Graz, 1976

moments of second order are dealt with. Green's function in the correlation terms is determined by using a n-group diffusion equation, which is decoupled by means of a principle axis transformation after having applied a Laplace transformation. In the transformed system the demanded Green's functions can be easily stated in form of bilinear developments.

5. Electromagnetic Wave Propagation in Plane Plasma Layers Subjected to Uniform Static Magnetic Field of Arbitrary Direction*

E.Ledinegg, B.Schnizer

To find the field representation of the electromagnetic field in an anisotropic plasma, it is necessary to calculate the mode continuum in infinite space, which requires the solution of the dispersion equation. This is a fourth order equation. The twodimensional case, in which the electromagnetic field depends only on two coordinates and the quartic becomes biquadratic, is an approximation sufficient in many practical casis. At first the corresponding system of modes and the integral representation of the electromagnetic field are given for only one plasma layer. Then the transition to a multiple-layer plasma requires the matching of tangential field components along the boundary, which task can easily be accomplished by solving a system of linear equations.

6. Wave Propagation in Plane Waveguides in an Anisotropic Plasma with Given Primary Current Distribution**

E.Ledinegg, W.Papousek

A multi-layered plasma is considered, where each layer becomes anisotropic by an arbitrary oriented static magnetic field. Wanted is an integral representation of the electromagnetic field excited by an arbitrary source distribution in the stratified plasma. Our method is similar to that of ARBEL and FELSEN, but extends the latter by assuming arbitrarily oriented static magnetic fields. The electromagnetic field is given as an integral representation, constructed from the modes of the transversal parts of the field equations. In case of a nonlinear interaction between plasma and electromagnetic field the obtained solution can be taken as a first order approximation to develope an iteration technique for the equations of magnetohydrodynamics.

7. A Diffusiontheoretical Method for the Flux Calculation in Multisphere Configurations

F.Schürrer

---

* Int.Congr. "Waves and Instabilities in Plasmas" Book of Abstracts, University of Innsbruck, 1975

** Kleinheubacher Berichte, Vol. 19, 1975

Starting from the exactly solvable problem of the flux determination of a point source of neutrons in an infinite medium, which contains a spherical impurity zone eccentric to the point source, an approximation method for the calculation of the flux distribution of two neighbouring spherical fuel elements in infinite diffusion media is developed. An iterative method allows by alternately satisfying the conditions of continuity of the two spherical fuel elements to proceed to continually improving approximations.

8. On the Calculation of the Doppler-effect of Reactor Materials

M.Heindler

A weak point in the safety analysis of fast breeders is the defective knowledge of the temperature effects on materials of medium atomic weight (60 volume % in fast breeders) that have a direct and indirect influence on the results of the calculations of the Doppler coefficient. The results derived from a quantum mechanical reactorphysical investigation of the relations between resonance structures of reaction rates and temperature effects show up the weak points of the usual calculation methods.

9. Neutron Physical Study on a Light Water Pebble Bed Reactor*

M.Heindler

The advantages of the pebble bed reactor, which have already been demonstrated in practice for the gas-cooled high temperature reactor, suggested the investigation of this principle for the application in reactors with liquid cooling as well. The results of various studies make pebble bed cores also for liquid cooled reactors appear as an interesting alternative to conventional core principles. On the basis of a parameter study of the neutron physical qualities of a pebble bed reactor with liquid cooling especially the neutron physical and thermodynamic characteristics of the fuel elements are discussed after describing the calculation methods. Unsolved problems are referred to.

10. Pulsed Neutron Source Measurements at the SAR Graz

W.Ninaus

Von Dardel suggested to determine the prompt kinetic behaviour of sub-critical assemblies with the help of the pulsed neutron tech-

---

* ATW, 11, p.574 - 580, Nov. 1975

nique. For applying this method, a pulsed neutron source for the installation in the central channel of the SIEMENS-ARGONAUT-Reactor in Graz has been designed and constructed. The principle of this pulsed neutron source is based on the periodical short utilization of the (γ,n) reaction in beryllium. The prompt neutron life time 1_o was determined with the method of Simmons and King. For the two core configurations, two-slab and ring-core, the measured values were compared with the results from the Rossi-α-measurements (Stribel and Thury).

11. A Contribution to the Measurement of the Neutron Flux with Wire Probes

Hj.Müller

For the determination of the neutron flux in reactors generally the induced beta and gamma activity will be measured in disk probes. At large flux profiles, the use of wire probes is advantageous, because by only one activation a very large field of the profile is determined. Sometimes it is possible to point out the fine structures of the flux, depending on the evaluation method. The results of the measurements will be discussed according to the evaluation of the beta and gamma activity as well as to the limits of the accuracy.

NETHERLANDS ENERGY RESEARCH FOUNDATION
ECN

Progress Report for the Period 1 January 1977 until 1 July 1978 of the Nuclear Data and Related Nuclear Physics Activities at the Energy Research Centre at Petten (The Netherlands).

Petten, July 18, 1978.

Fission-Product Nuclear Data Project (compiled by H. Gruppelaar)

1. Introduction

The purpose of the Dutch Fission-Product Nuclear Data (FPND) project is to obtain neutron cross sections for the prediction of the effects of fission products in large fast power reactors. For this purpose neutron cross sections are evaluated from which 26-group constants are calculated and adjusted to fit integral measurements, performed at STEK (Petten) and CFRMF (Idaho). Recently, adjustment have been applied also to evaluated point cross sections. The project is performed in the framework of a cooperation between Germany, Belgium and The Netherlands on fast breeder reactor development. The progress of the project is reported in quarterly reports |1-3|.

In 1977 a great deal of effort has been devoted to prepare a contribution |4| and two reviews |5,6| for the Second I.A.E.A. Advisory Group Meeting on FPND which was held at Petten, September 5-9, 1977. It appeared that the contribution of integral measurements to the present status of fast fission-product capture cross sections was rather important. For most nuclides the requested accuracy could only be reached by using these data in an adjustment process. The contribution of STEK integral data was very significant: in most cases the requirements were met already without the use of other integral experiments.

2. Evaluation of neutron cross sections (microscopic point data)

In refs. |7,8| neutron cross sections are given for 34 fission products, evaluated in 1975 to 1977. The most recent evaluations, yet to be published, are those for the Nd isotopes and for ^{147}Pm. The complete list of nuclides for which the so-called RCN-2 evaluation has been completed is given below: ^{93}Nb, $^{92,94,95,96,97,98,100}Mo$, ^{99}Tc, $^{101,102,104}Ru$, ^{103}Rh, $^{102,104,105,106,107,108,110}Pd$, $^{107,109}Ag$, $^{127,129}I$, ^{133}Cs, ^{139}La, ^{141}Pr, $^{142,143,144,145,146,147,148,150}Nd$, ^{147}Pm, $^{147,148,149,150,151,152,154}Sm$. New evaluations are in progress for the stable Eu isotopes. For the capture cross sections the un-

certainty margins and correlation coefficients have been evaluated as well. These results have not been published, but the uncertainty margins of the group constants are given in refs. |14,15|. The format of the evaluated microscopic data files is that of the KEDAK library. These files are available from the NEA Data Bank at Saclay.

Adjusted microscopic cross section evaluations based upon the RCN-2 evaluation and integral measurements in STEK and CFRMF have been obtained by utilizing adjusted statistical-model parameters for a recalculation of the capture cross sections above 1 keV. These data have been obtained so far for 13 nuclides: ^{99}Tc, ^{103}Rh, $^{107,109}Ag$, $^{127,129}I$, $^{147,148,149,150,151,152,154}Sm$.

Recently, a new evaluation of natural Mo cross sections has been completed, containing revised radiative capture data |9| which give about 16% lower average capture cross sections in a fast breeder reactor than the currently used ENDF/B-IV and KEDAK-3 cross sections. The new evaluation |10| is in very good agreement with STEK integral reactivity worths for natural Mo. The data file is available from the NEA Data Bank at Saclay.

Some work has been devoted to the theory of the width fluctuation correction factor used in the statisitcal model, in cooperation with CNEN, Bologna |11|. Other theoretical work has been performed on the pre-equilibrium model |12,13|.

3. Adjustment of 26-group constants and neutron spectra

Unadjusted and adjusted capture group constants (with uncertainties) based upon the RCN-2 evaluation |7,8| and integral STEK reactivity worths have been published in refs. |14,15|. For those nuclides, for which CFRMF activation measurements are also available, both STEK and CFRMF results have been used to obtain adjusted group constants |4|. An outline of some results is given in conference reports |16, 17| and in Table 1. Very recently also adjustment calculations have been performed for the capture cross sections of the stable Nd isotopes and for ^{147}Pm.

The adopted method of adjustment has been described in ref. |18|. This method has also been used for the adjustment of STEK flux and

adjoint flux spectra. For this purpose rather complete 26x26 spectrum co-variance matrices have been calculated, based on assumed basic nuclear data uncertainties |19|. These adjusted STEK spectra have been used to calculate all published results of FPND adjustments |4,5,6,14,15|. Reports on experimentally determined STEK spectra have been given in refs. |20,21|.

4. References

|1| Hoekstra, E.K. Fast reactor programme, First quarter 1977 progress report. ECN-22 (1977).

|2| Hoekstra, E.K. Fast reactor programme, Combined second and third quarter 1977 progress report. ECN-34 (1977)

|3| Hoekstra, E.K. Fast reactor programme, Fourth quarter 1977 progress report. ECN-41 (1978).

|4| Dekker, J.W.M. and H.Ch. Rieffe. Adjusted capture cross sections of fission-product nuclides from STEK reactivity worths and CFRMF activation data. ECN-28 (1977).

|5| Gruppelaar, H. and J.W.M. Dekker. Impact of integral measurements on the capture cross section evaluations of individual fission product isotopes. ECN-24 (1977).

|6| Bustraan, M. et al. Integral determination of fission-product neutron capture cross sections for application in fast reactors. ECN-27 (1977).

|7| Gruppelaar, H. Tables of RCN-2 fission-product cross section evaluation, vol. 1 (24 nuclides). ECN-13 (1977).

|8| Gruppelaar, H. Tables of RCN-2 fission-product cross section evaluation, vol. 2 (13 nuclides), ECN-33 (1977).

|9| Gruppelaar, H. and J.W.M. Dekker. Evaluation and adjustments of radiative capture cross sections of natural Mo and the stable Mo isotopes. Proc. Specialist Mtg. on Neutron Data of Structural Materials for Fast Reactors, Geel, Belgium, Dec. 5-8, 1977.

|10| Gruppelaar, H. Evaluated neutron cross sections of natural molybdenum. ECN-40 (1978).

|11| Gruppelaar, H. and G. Reffo. Some properties of the width fluctuation factor, Nucl. Sci. and Eng. 62 (1977) 756.

|12| Luider, F.J. Pre-equilibrium theory and slaves of the master equation, ECN-17 (1977).

|13| Luider, F.J. Note on the solution of the master equation in the exciton model. Z. Physik A284 (1978) 187.

|14| Dekker, J.W.M. Tables and figures of adjusted and unadjusted capture group cross sections based on the RCN-2 evaluation and integral measurements in STEK, vol. 1, ECN-14 (1977).

|15| Dekker, J.W.M. Tables and figures of adjusted and unadjusted capture group cross sections based on the RCN-2 evaluation and integral measurements in STEK, vol. 2, ECN-30 (1977).

|16| Dekker, J.W.M. et al., Fission-product capture cross sections for a fast breeder reactor. Proc. Reaktortagung 1977, Mannheim, March 1977, ZAED, Karlsruhe, p. 87 (1977).

|17| Gruppelaar, H. et al. Neutron capture cross section adjusment based upon integral measurements, Trans. Am. Nucl. Soc. 27 (1977), p. 876.

|18| Dragt, J.B. et al. Methods of adjustment and error evaluation of neutron capture cross sections; application to fission product nuclides. Nucl. Sci. and Eng. 62 (1977) 117.

|19| Dekker, J.W.M. et al. Neutron spectra of STEK cores for reactivity calculations. ECN-35 (1977).

|20| Montizaan, J. and H. Ames. Fast neutron spectrum measurements with a proton recoil spectrometer in the fast-thermal coupled critical facility STEK. ECN-26 (1977).

|21| Oei, T.D. et al. Time-of-flight measurements in STEK. ECN-19 (1977)

Table 1

AVERAGE CAPTURE CROSS SECTIONS (IN b) AND THEIR STANDARD DEVIATIONS FOR SOME IMPORTANT F.P. NUCLIDES (SNR-300 FLUX SPECTRUM).

Nuclide	RCN-2 [7,8] (unadjusted)	RCN-2A [14,15] STEK	RCN-2A [4] CFRMF	RCN-2A [4] STEK+CFRMF	ENDF/B-IV
^{95}Mo	0.30 (18%)	0.28 (8%)	-	-	0.29
^{97}Mo	0.30 (17%)	0.30 (9%)	-	-	0.28
^{98}Mo	0.086 (9%)	0.084 (9%)	0.088 (6%)	0.087 (6%)	0.101
^{100}Mo	0.10 (27%)	0.080 (21%)	0.074 (9%)	0.074 (8%)	0.078
^{99}Tc[a]	0.54 (16%)	0.64 (7%)	0.49 (10%)	0.59 (6%)	0.49
^{101}Ru	0.69 (16%)	0.68 (8%)	-	-	0.53
^{102}Ru	0.20 (35%)	0.15 (18%)	0.15 (10%)	0.16 (8%)	0.19
^{104}Ru	0.17 (30%)	0.14 (10%)	0.14 (9%)	0.14 (7%)	0.14
^{103}Rh[a]	0.64 (9%)	0.64 (6%)	0.64 (9%)	0.64 (6%)	0.70
^{105}Pd	0.81 (16%)	0.88 (7%)	-	-	0.83
^{107}Pd	0.96 (55%)	0.93 (10%)	-	-	0.57
^{108}Pd	0.18 (85%)	0.17 (19%)	0.17 (30%)	0.17 (17%)	0.16
^{109}Ag	0.68 (12%)	0.71 (7%)	0.74 (8%)	0.73 (6%)	0.48
^{127}I [a]	0.52 (9%)	0.57 (7%)	0.50 (8%)	0.57 (7%)	0.54
^{129}I	0.34 (25%)	0.30 (12%)	0.30 (9%)	0.30 (8%)	0.38
^{133}Cs	0.51 (12%)	0.51 (7%)	0.46 (6%)	0.49 (6%)	0.48
^{139}La	0.031 (16%)	0.035 (12%)	0.030 (8%)	0.031 (7%)	0.038
^{141}Pr	0.13 (12%)	0.12 (8%)	0.12 (8%)	0.12 (7%)	0.16
^{143}Nd[b]	0.32 (8%)	0.30 (7%)	- -	-	0.30
^{145}Nd[b]	0.46 (9%)	0.48 (7%)	-	-	0.33
^{146}Nd[b]	0.093(15%)	0.090(15%)	0.092 (10%)	0.091 (9%)	0.13
^{148}Nd[b]	0.14 (11%)	0.13 (11%)	0.14 (8%)	0.14 (8%)	0.18
^{150}Nd[b]	0.18 (10%)	0.17 (10%)	0.17 (10%)	0.16 (9%)	0.22
^{147}Pm[b]	1.04 (19%)	1.30 (8%)	1.15 (12%)	1.28 (7%)	1.25
^{149}Sm	2.24 (15%)	2.21 (9%)	-	-	1.41
^{151}Sm	2.13 (9%)	1.80 (14%)	-	-	2.21
^{152}Sm	0.41 (12%)	0.47 (9%)	0.42 (6%)[b]	0.44 (5%)[b]	0.40

a) Revised RCN-2 evaluation.

b) Recent results, not yet published.

The Study of the (n,γ) Reaction (compiled by K. Abrahams)

A. New instrumentation

1. Filtered neutron beam at H.F.R.

For one of the large channels at the research reactor H.F.R. a filter of natural iron with some sulfur and aluminium has been set-up to obtain a 24 keV neutron beam. Measurements have been performed on the reactions Mn(n,γ) and Ni(n,γ).
The filtered beam has an intensity of about 10^6 neutrons/second and an energy spread of 5 keV.

2. Nuclear orientation facilities

a) A design is being made for a new nuclear orientation facility in which, by use of the method of nuclear demagnetisation and application of a superconducting magnet a magnetic field of 10 T and temperatures of 10 mK will be reached. In this way it will be possible to polarise by brute force most odd A nuclides, which are in a metallic lattice.

b) In the existing facility the formerly used neutron monochromator CoFe crystal is exchanged for a Heusler crystal for which the neutron polarisation P_n is 95% and the intensity has risen from 6.10^5 to 4.10^6 neutrons per second.
It has been verified by measurements on the V(n,γ) reaction that the figure of merit $P_n^2 I$ has been increased accordingly.

B. Measurements

1. Measurements on light nuclei (sd shell)

The reactions $^{23}Na(n,\gamma)$, $^{27}Al(n,\gamma)$, $^{31}P(n,\gamma)$ and $^{35}Cl(n,\gamma)$ have been studied on direct and semi-direct components by measurements with polarised neutrons and by measuring the angular correlation of the capture γ's. New measurements have been performed on the mixing of spins in the capture state.
In Al(n,γ) and E1(M2) mixing of the order of one percent has been observed, and in $^{23}Na(n,\gamma)$ an M1(E2) mixing of the order of 10 percent.

2. Measurements on medium weight nuclei (fp shell)

Measurements have been finished on ^{43}Ca, ^{45}Ca, ^{46}Sc, ^{47}Ti, ^{52}V, ^{56}Mn, ^{59}Fe, ^{65}Ni, ^{65}Zn, ^{67}Zn, ^{69}Zn and ^{71}Zn.
On most of these isotopes shell model calculations (surface delta interaction method) are being performed in cooperation with the R. v.d. Graaff Laboratory of the State University of Utrecht. Also in the analysis of some Zn isotopes excitation energies have been established with an accuracy of 100 eV.

3. Study of some nuclides with about 82 neutrons

Measurements on ^{137}Ba, ^{139}Ba, ^{141}Ce, ^{143}Ce, ^{143}Nd and ^{145}Nd have been finished. Nuclear orientation and γ-polarisation measurements were performed on ^{141}Pr for which a preliminary analysis has been made.

C. Publications

K. Abrahams, Isobaric Spin Interference in the Neutron Capture State. (Proceedings of the ICNS, Tokyo 1977, p. 137).

J. Kopecky, Average Photon Strength for Mass Range A <50. (Ibid. p. 78).

C.F. Clement, A.M. Lane and J. Kopecky, Correlations in M1 Capture as Evidence for a Semi-Direct Mechanism (Phys. Lett. B71 (1977) 10).

J.J. Bosman and H.Postma, Spin assignments in low energy neutron capture reactions using polarized neutrons and oriented target nuclei. Nucl. Instr. and Meth. 148 (1978) 331.

R. Vennink, W. Ratynski and J. Kopecky, Circular polarization of neutron capture γ-rays from Ca, Ti, Fe and Ni.
Nucl. Phys. A299 (1978) 429.

J. de Boer, Precise excitation energies in ^{65}Zn resulting from slow neutron capture in ^{64}Zn. ECN-78-037.

S. Barkan, Study of ^{28}Al by $^{27}Al(n,\gamma)$ reaction.
FYS-KF-78-01.

A. Girgin, Circular polarization of neutron capture γ-rays from $^{27}Al(\vec{n},\vec{\gamma})^{28}Al$ reaction. ECN-78-088.

NEANDC (OR) - 151"L"
Part B
INDC (SWT) - 12 / G

PROGRESS REPORT TO NEANDC FROM SWITZERLAND

June 1978

T. Hürlimann

Swiss Federal Institute for Reactor Research
Würenlingen

NOT FOR PUBLICATION

PREFACE

This document contains information of a preliminary or private nature and must be used with discretion. Its contents may not be quoted, abstracted, reproduced, transmitted to libraries or societies or formally referred to without the explicit permission of the originator.

CONTENTS

I. Institut de Physique, Université de Neuchâtel

(Dir.: Prof. Jean Rossel)

1. n-d elastic differential cross section at 2.48 and 3.38 MeV

P. Chatelain, Y. Onel and J. Weber

In 1977, we have completed the analysis of the data from the experiments described in the previous report. Preliminary results of these experiments have been published {1}. A detailed description of the method which we have used to measure the response and the resolution of the scatterers have also been published {2}. The final results will be soon submitted for publication. As we have expected, the partial waves higher than $\ell = 2$ are needed to fit forward angles data {3} and our data ($-1. \leq \cos \theta_{CM} \leq +0.5$). Phase shifts analyses of these data are in progress.

References

{1} P. Chatelain et al., Helv. Phys. Acta. Accepted for publication

{2} P. Chatelain et al., Nucl. Inst. Meth. Accepted for publication

{3} J. D. Seagrave et al., Phys. Rev. 105 (1957) 1816

2. Depolarization factor D(θ) for the $d(\vec{n},\vec{n})d$ reaction at 2.45 MeV

D. Bovet, P. Chatelain, Y. Onel and J. Weber

We hope to complete the measurements of the angular variation of D by the end of this year. The results of these measurements will be of great help in the better understanding of the doublet phase shifts for this reaction. Part of our results for D(θ) have already been published {1} as well as our results for A(θ) which had been previously obtained {2}.

Our cross section D(θ)- and A(θ)-results will be soon used as input data to extensive effective range {1} and phase shifts analyses.

{1} D. Bovet et al., J. of Physics G. Accepted for publication

{2} D. Bovet et al., Proceedings of the ICINN-Conference, Lowell 1976, part 2, p. 1357 (CONF - 760715-p2)

3. Three body reactions with ^{6}Li

F. Foroughi, E. Bovet, C. Nussbaum and B. Vuilleumier

During the last year, we measured the α-α quasifree scattering (QFS) in the ^{6}Li (α,αα)d reaction at 59 MeV. The purpose of this experiment is to remove the kinematical degeneracy {1}.

Our measurement was monitored with the elastic reaction ^{6}Li (α,α)^{6}Li, which we measured with high accuracy (see fig. 1). These data are analysed with an optical potential. In order to match our data to the previously reported ones {2}, we repeated the measurement for three configurations ($\theta_1 = -\theta_2 = 44{,}15$, $\theta_1 = 35{,}15$, $\theta_2 = -53{,}1$ and $\theta_1 = 29{,}15$, $\theta_2 = -58{,}9$).

Our results do not agree with those quoted in {2} (see fig. 2). The critical configuration is that with $\theta_{CM} = 72^0$ ($\theta_1 = 35{,}15$, θ_2 53,1). If this result is confirmed, the mechanism would be then a final state interaction instead of a QFS one.

References

{1} E. Bovet, F. Foroughi, C. Nussbaum, B. Vuilleumier and J. Rossel, SIN Jahresbericht 1977, page E89

{2} J.W. Watson, H. G. Pugh, P. G. Roos, D. A. Goldberg, R. A. Riddle and D. I. Bonbright, Nucl. Phys. A172 (1971) 513

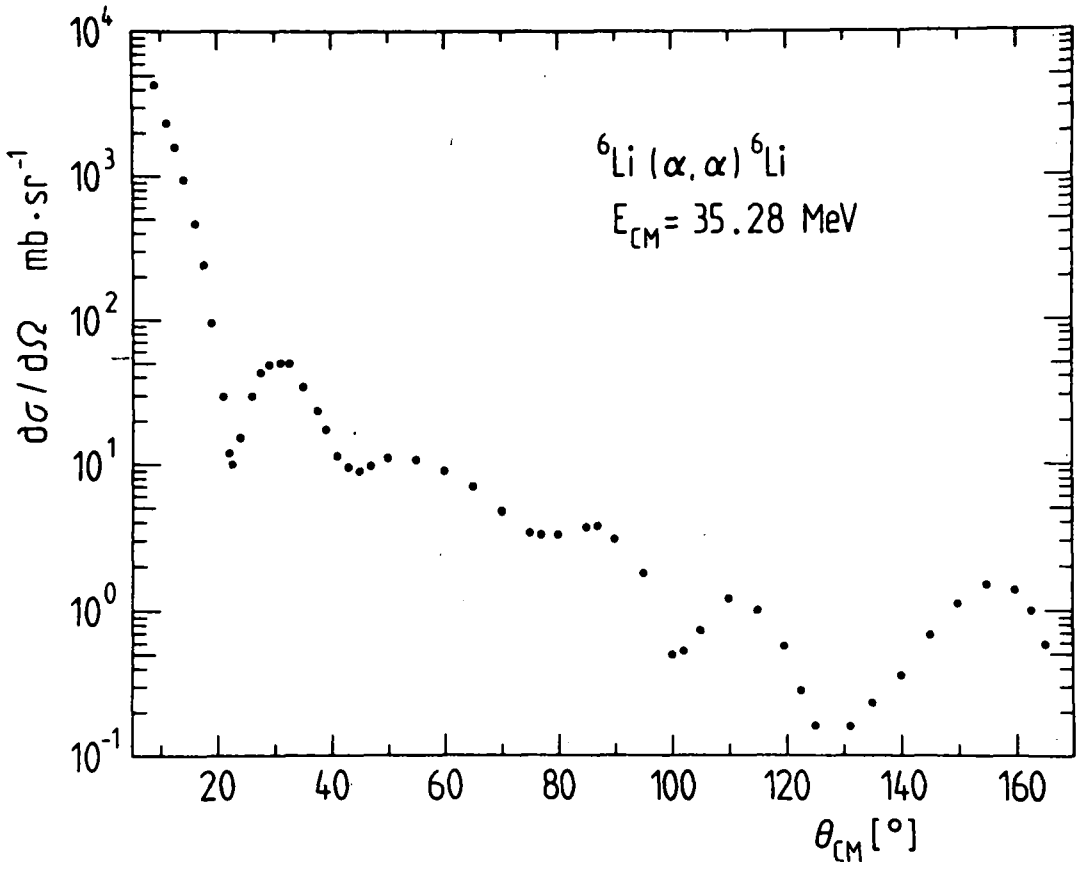

Fig. 1: Measured α-^{6}Li elastic cross section. The points are larger than the error bars.

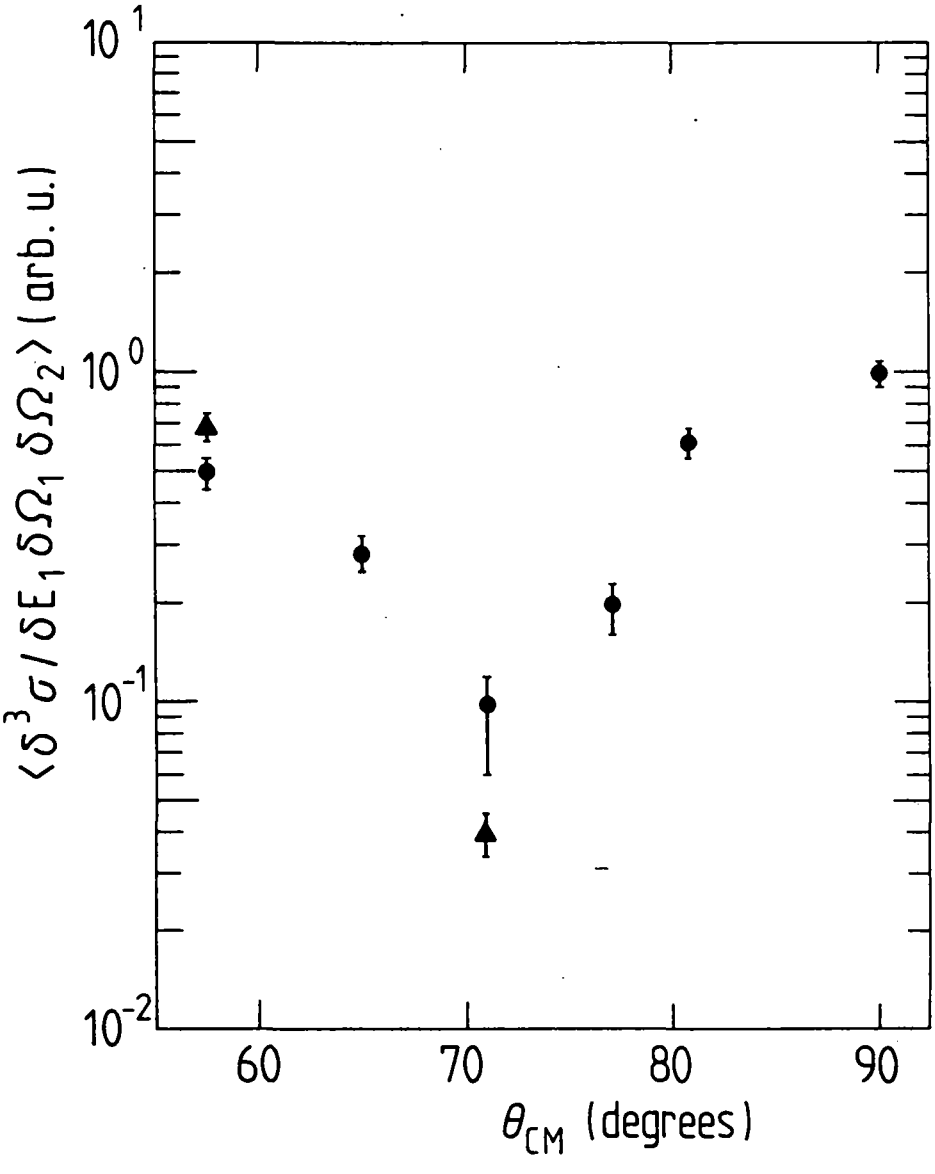

Fig. 2: QFS peak cross section for various configurations. Our data (triangle) were normalized to those of Watson {2} at $\theta_{CM} = 90^0$.

II. Eidg. Institut für Reaktorforschung, Würenlingen

Dir.: Prof. Dr. H. Gränicher

1. Independent yields of ^{148m}Pm and ^{148g}Pm in the thermal neutron-induced fission of ^{233}U and ^{239}Pu

H. U. Zwicky and H. R. von Gunten

Pm was separated from rare earths fission products using high pressure ion exchange chromatography (Aminex A5 cation exchanger, α-hydroxiisobutyric acid with pH gradient). The samples were measured with Ge(Li)-γ-ray spectroscopy ralative to ^{151}Pm and ^{149}Pm. The independent and fractional independent yields for ^{148m}Pm and ^{148g}Pm are shown in table 1.

Table 1: Independent and fractional independent yields for ^{148m}Pm and ^{148g}Pm in the thermal neutron-induced fission of ^{233}U and ^{239}Pu

Target nuclide	Independent yield (%)		Fractional independent yield (%)	
	^{148m}Pm	^{148g}Pm	^{148m}Pm	^{148g}Pm
^{233}U	$(7.8\pm1.4)\times10^{-7}$	$(1.8\pm0.4)\times10^{-7}$	$(6.1\pm1.1)\times10^{-7}$ [a]	$(1.4\pm0.3)\times10^{-7}$ [a]
^{239}Pu	$(4.3\pm0.7)\times10^{-6}$	$(1.3\pm0.3)\times10^{-6}$	$(2.6\pm0.4)\times10^{-6}$ [b]	$(7.9\pm1.7)\times10^{-7}$ [b]

a) Yield of chain 148: (1.271±0.006)% {1}

b) Yield of chain 148: (1.636±0.008)% {1}

Reference

{1} Meek and Rider, NEDO-12154

2. Spontaneous-fission half-lives of ^{234}U and ^{236}U

H. W. Reist and M. Baggenstos

The partial spontaneous-fission half-lives of ^{234}U and ^{236}U have been re-measured using the rotation chamber. The highly enriched uranium isotopes (^{234}U: 99.37 w/o; ^{236}U: 99.685 w/o) were loaned from the Argonne National Laboratory.

To reduce neutron induced fission the experiment was surrounded by 20 cm paraffin containing 16 w/o boron.

The following values were obtained:

$$^{234}U : T_{1/2} \text{ (sp. f.)} = (1.42 \pm 0.10) \times 10^{16} \text{ years}$$

$$^{236}U : T_{1/2} \text{ (sp. f.)} = (2.43 \pm 0.17) \times 10^{16} \text{ years}$$

3. Radiochemical investigation of the mass distribution and probability in stopped μ^- induced fission of ^{238}U

P. Baertschi, A. Grütter, H.R. von Gunten, H.S. Pruys*, M. Rajagopalan**, H.W. Reist and E. Rössler

Radiochemical measurements of 24 fission products show that the mass-split is asymmetric in stopped μ^- induced fission of ^{238}U. The mass distribution is similar to 14 MeV neutron-induced fission. The main difference is a smaller peak-to-valley ratio indicating a mean excitation energy of about 20 MeV. The fission probability (prompt and delayed) is 0.15±0.03 per stopped muon.

For details confer publication in Nuclear Physics A294 (1978) 369.

* University of Zürich, Switzerland

** Chem. Div., Stony Brook University, New York

4. Half-life of ^{57}Mn

A. Wyttenbach, A. Schubiger, H.S. Pruys*

^{57}Mn and ^{58}Mn were produced by the reaction ^{59}Co (μ^-, p)^{58}Mn and ^{59}Co (μ^-, pn)^{57}Mn in the same target and their half-lives determined by gamma-ray-spectroscopy. The value for ^{58}Mn was found to be (65 ± 1)s in perfect agreement with literature values; contrarily the value for ^{57}Mn was found to be (86.7 ± 0.8)s, what is considerably less than previously reported values.

* University of Zürich, Switzerland

III. Laboratorium für Kernphysik, Eidg. Technische Hochschule, Zürich

(Dir.: Prof. Dr. J. Lang)

1. Elastic Scattering and neutron-transfer reactions with ^{9}Be

L. Jarczyk, B. Kamys, J. Lang, R. Müller, E. Ungricht and J. Unternährer

The elastic scattering of ^{9}Be on ^{9}Be, ^{12}C, ^{16}O and seven heavier target nuclei in the mass region between ^{24}Mg and ^{197}Au was measured at beam energies of 14, 20 and 26 MeV. In a sputtering ion source a BeO^{-} beam was produced, accelerated up to the terminal of the Tandem accelerator and converted to positive Be-ions in a gas stripper {1}.

The angular distributions of the scattering on light nuclei show distinct diffraction patterns. Calculations with fitted optical potentials give good agreement with the measurements on ^{12}C target in the angular range $\theta_{cm} < 90^{0}$ only. It seems that at bigger angles elastic transfer processes (^{3}He-transfer) are important.

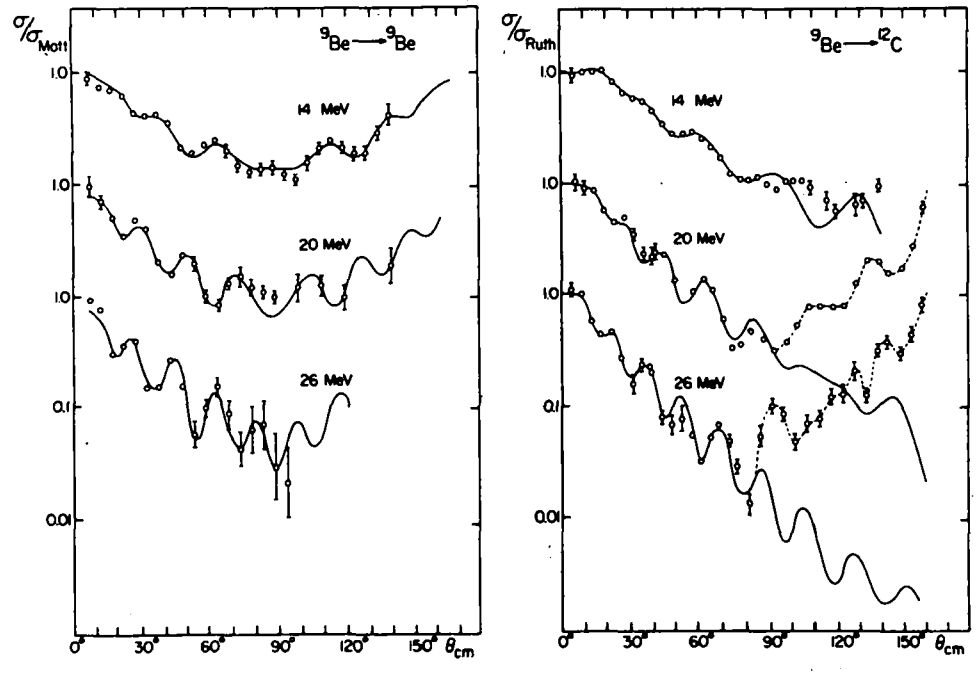

Fig. 1: Angular distribution of elastic scattering of ^{9}Be on ^{9}Be and ^{12}C. Solid lines: Optical model calculations. The dotted lines are only for guiding the eye.

The angular distributions of the scattering on heavier target nuclei could be reproduced at all angles and all energies by optical model calculations. The potentials were calculated with the Ansatz

$$U = V_c - (V_0 + iW_0)/f(r)$$
$$f(r) = 1 + \exp\{(r - R_n)/a\}$$
$$R_n = R_0 \cdot (A_t^{1/3} + A_b^{1/3}) - R_1$$

where the Coulomb potential was approximated by

$$V_c = \frac{Z_t Z_b e^2}{r} \qquad r \geq R_c$$
$$V_c = \frac{Z_t Z_b e^2}{2R_c}\left(3 - \left(\frac{r}{R_c}\right)^2\right) \qquad r \leq R_c$$
$$R_c = R_{c0} \cdot A_t^{1/3} \qquad R_{c0} = 1.2\ \text{fm}$$

It was possible to find a universal potential reproducing all angular distributions with good agreement. Because of the existence of an ambiguity the depth V_0 of the real potential was fixed and the other parameters fitted. The obtained values are listed in table 1. Compared with other heavy ion potentials the great diffusiveness a and the big ratio W/V ≈ 2 are remarkable.

Table 1: Optical model parameters for elastic scattering of ^{9}Be on targets from ^{24}Mg to ^{197}Au

V_0	2.5	5.0	10.0	20.0	40.0	69.0	MeV
W_0	7.6 ± 0.3	11.8 ± 0.5	20.4 ± 0.8	37.5 ± 1.5	72.7 ± 2.8	130.0 ± 3.5	MeV
a	0.73 ± 0.01	0.78 ± 0.01	0.82 ± 0.01	0.85 ± 0.01	0.87 ± 0.01	0.89 ± 0.01	fm
R_0	1.26 ± 0.02	1.31 ± 0.02	1.34 ± 0.02	1.36 ± 0.02	1.37 ± 0.02	1.36 ± 0.02	fm
R_1	−0.83 ± 0.08	0.06 ± 0.09	0.91 ± 0.10	1.71 ± 0 10	2.45 ± 0.10	3.00 ± 0.10	fm
χ^2	2.13	1.90	1.83	1.83	1.84	1.90	

In addition, neutron-transfer reactions on ^{28}Si and ^{40}Ca targets leading to different bound states of ^{29}Si and ^{41}Ca were measured. The angular distributions were compared with finite range DWBA calculations. Unfortu-

nately it was not possible to extract spin values for the levels in the final nuclei ^{29}Si and ^{41}Ca since the results are only weakly spin dependent. From levels with known spins and using known spectroscopic factors for these levels, a spectroscopic factor for ^{9}Be can be determined. The value found in this way amounts to $S(^{9}Be \rightarrow {}^{8}Be + n) = 0.42 \pm 0.04$; it is lower than the theoretical value $S_{th} = 0.58$, though the accuracy of the latter is around 20 % {2}. The DWBA analysis is not sensitive to the optical model parameters as long as they reproduce well the elastic scattering.

References

{1} R. Balzer, Proc. Europ. Conf. on Nuclear Physics with Heavy Ions, Caen 1976

{2} S. Cohen and D. Kurath, Nucl. Phys. A101, 1 (1967)

2. Comparison of the mirror reactions $^{2}H(d,p)^{3}H$ and $^{2}H(d,n)^{3}He$

V. König, W. Grüebler, R.A. Hardekopf, B. Jenny, R. Risler and H.R. Bürgi

In previous comparisions of the polarizations of the outgoing nucleons in the mirror reactions $^{2}H(d,p)^{3}H$ and $^{2}H(d,n)^{3}He$ it was shown {1,2} that the proton polarizations are larger than the neutron polarizations. These sizable differences can be removed by lowering the deuteron energy for the (d,n) reaction by 1.5 MeV {1,2} to give a comparison for the same energy in the exit channels. To investigate similar effects in the analysing powers the observables iT_{11}, T_{20}, T_{21} and T_{22} were measured for both reactions with high precision in steps of 1.5 MeV between 2.5 and 11.5 MeV. The angular range of comparison is restricted to backward angles mainly by the experimental technique used for measuring the recoil ^{3}He for the (d,n) reaction. The experimental results have been fitted with Legendre polynomials. Fig. 1 compares the results of the (d,p) reaction with the fits of the mirror reaction at the same deuteron energy and shows discrepancies for T_{20} and T_{22}.

Fig. 2 compares the results of the (d,n) reaction with the fits of the (d,p) reaction at the same energy in the exit channels and shows better agreement for T_{20} and T_{22}, but strong deviations for iT_{11} and T_{21}. For a better overall comparison, the following average deviation is given in Fig. 3:

$$D_{av} = \int_{\theta_1}^{\theta_2} D_{kq}(\theta)d\theta/(\theta_2-\theta_1)$$

where: $D_{kq} = |T_{kq}(d,p)-T_{kq}(d,n)|$ and $\theta_1 = 100^0$ and $\theta_2 = 160^0$. This figure shows that when the correction for the Coulomb displacement proposed in {1,2} is applied the discrepancies persist. These almost energy independent discrepancies are observed in a region where Coulomb effects ought to be small (low charge of all particles, large energy of the emitted nucleons, backward hemisphere of scattering) and therefore a violation of charge symmetry should not be excluded from consideration. Although at the present time it seems too difficult to filter out the Coulomb effects in a proper way, hopefully the future will show if a combination of strong forces with charge symmetry property and electromagnetic forces can explain the present results. Model calculations of the ^{4}He excitations e. g. multichannel R-matrix calculations, should be helpful in the investigation of this most important question.

References

{1} R.A. Hardekopf, R.L. Walter and T.B. Clegg, Phys. Rev. Lett. 28 760 (1972)

{2} R.A. Hardekopf et al., Nucl. Phys. A191, 468 (1972)

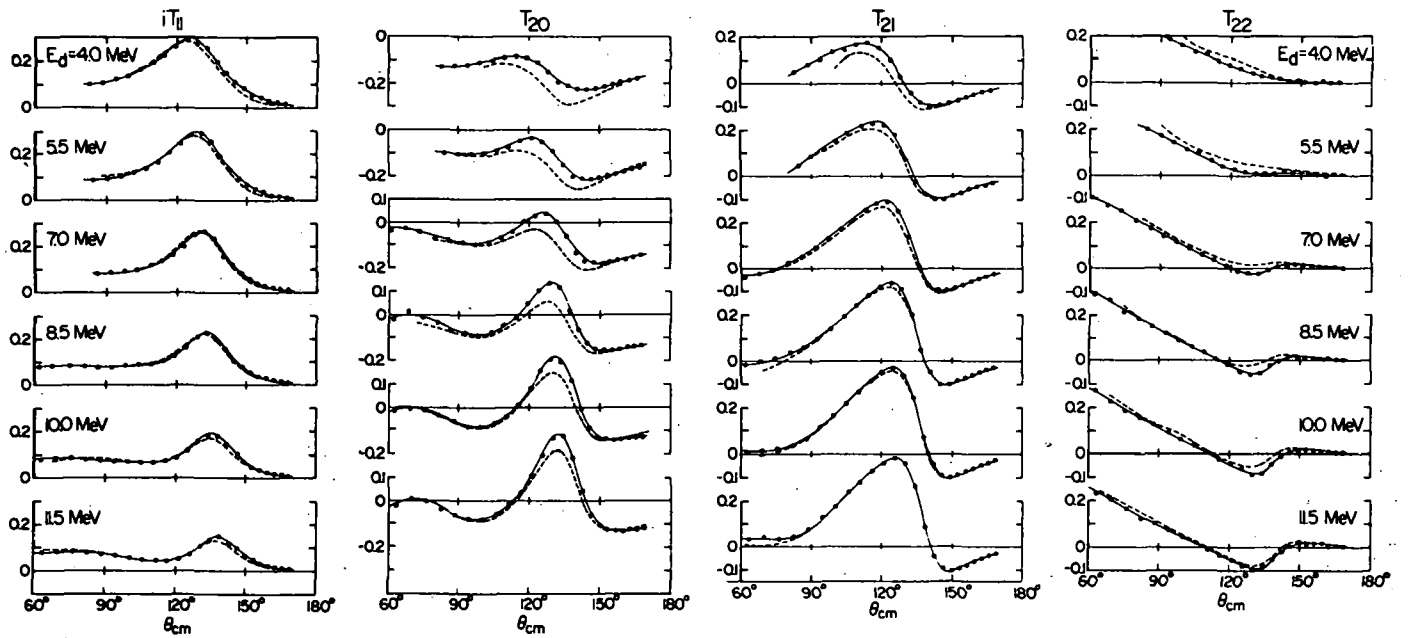

Fig. 1: Comparison of the analysing powers at the same deuteron energy. The dots are the results of the $^{2}H(d,p)^{3}H$ reaction, the solid curves fits to these data. The dashed curves are fits to the (d,n) reaction.

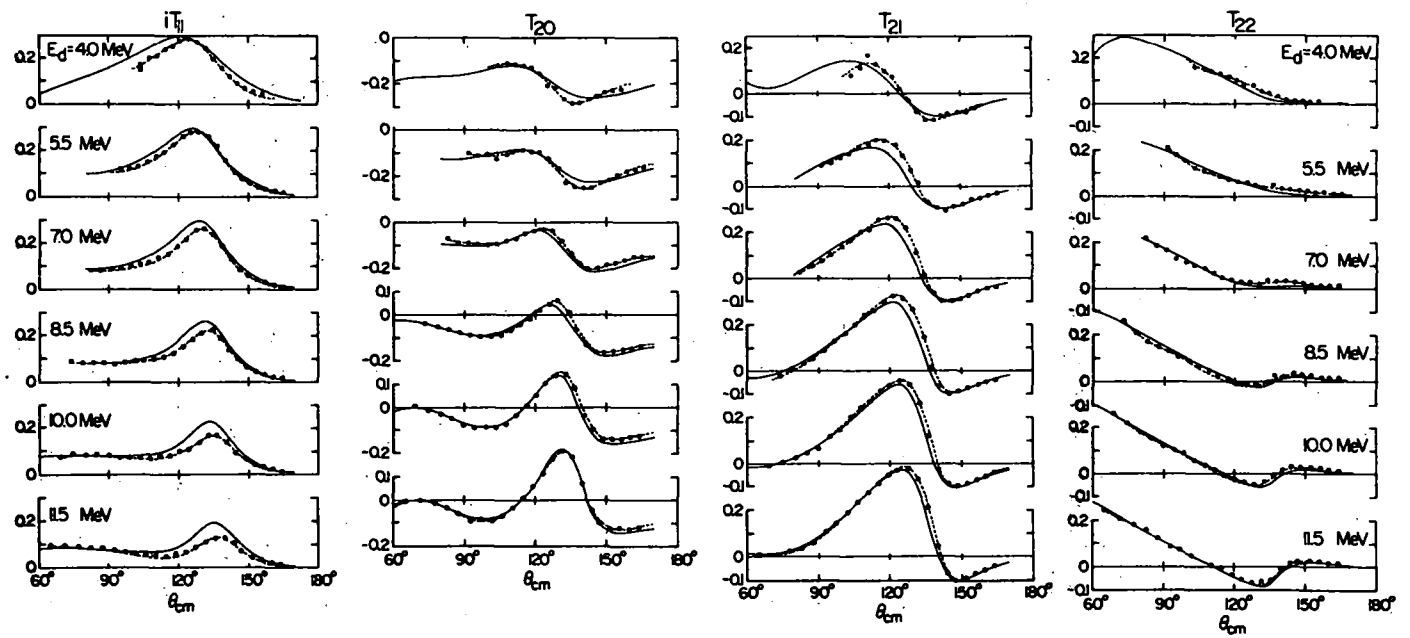

Fig. 2: Comparison of the analysing powers at the same exit energy of the nucleons. The dots are results of the $^{2}H(d,n)^{3}He$ reaction, the dashed curves fits to these data. The solid curves are fits to the (d,p) reaction, for deuteron energies lower by 1.5 MeV than the indicated energies.

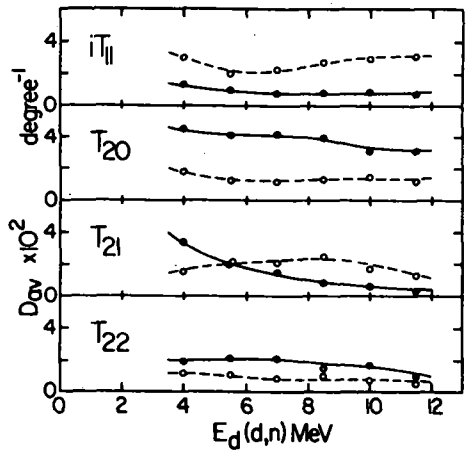

Fig. 3: Average deviation D_{av} of the analysing powers for the mirror reactions as a function of energy. The dots represent comparisons at the same entrance energies, the circles at the shifted energies. The solid and dashed lines are drawn to guide the eye. The size of the dots and circles indicates the uncertainties in D_{av}.